Optical Engineering

SPIEDigitalLibrary.org/oe

Background illumination regularization on interferograms

David L. Romero-Antequera
Dayana H. Penalver
Fermín-Salomón Granados-Agustín
Javier Sánchez-Mondragón

Background illumination regularization on interferograms

David L. Romero-Antequera
Dayana H. Penalver
Fermín-Salomón Granados-Agustín
Javier Sánchez-Mondragón
Instituto Nacional de Astrofísica, Optica y Electrónica
Calle Luis Enrique Erro No. 1 Tonantzintla
Puebla 72000, México
E-mail: dromero.fisica@gmail.com

Abstract. A method for background illumination regularization, which requires only one image and a single-stage correction, is presented. The method yields in the exact computation of the background illumination and the local visibility of the fringes from the envelopes of the intensity distribution. The approach is clear, elegant, and easy to implement. The results of the method are compared with another recent approximation, proving itself competitive enough. © *2012 Society of Photo-Optical Instrumentation Engineers (SPIE).* [DOI: 10.1117/1.OE.51.9.095601]

Subject terms: visibility; digital processing; image enhancement; image processing; interferometry; spatial filtering.

Paper 120739 received May 22, 2012; revised manuscript received Jul. 27, 2012; accepted for publication Jul. 30, 2012; published online Sep. 6, 2012.

1 Introduction

The interferometers are interesting devices used for the estimation of physical quantities. Among those quantities, there is the fringe pattern, which is a sinusoidal function of the phase variation. The computation of the phase, then, involves the inversion of a cosine function, whose result is a wrapped phase modulo 2π. This wrapped phase, although correctly reproduces the fringe pattern, does not correctly represent the wavefront under consideration. There is a large number of methods for phase unwrapping, i.e., the reconstruction of the wavefront from the data in the wrapped phase; however, independently of the method, a preprocessing (or spatial filtering[1]) of the acquired data should be carried out.

The background illumination suppression is a fundamental step in the analysis of interferometric images.[1–5] For several situations, the typical solution is the enhancement of laboratory conditions in order to obtain better contrast and/or homogeneous illumination. However, there are certain scenarios where it is not possible to change laboratory conditions, i.e., expensive data acquisition, postprocessing of dynamic phenomena, etc. In these situations, a suitable algorithm must be implemented in order to enhance the acquired images and suppress background illumination.

Probably, the best known method for achieving so was presented by Takeda[6] in a classical paper. The method yields on the manipulation of the Fourier spectra in order to identify both background illumination and spurious (noise) frequencies. This method has a major drawback: it is necessary for the scientist to identify such frequencies and filter them out. For an experienced user, this is a powerful tool, but it is clear that an automatic or semiautomatic method would do better in many situations.

Although this is an old problem, a new approach is published from time to time.[7–10] Quiroga et al.[7] presented an algorithm for fringe normalization using two orthogonal bandpass filters. Following this work, Quiroga and Servin[8] presented an approach, which is a direct and isotropic operator, based on the application of an n-dimensional quadrature transform. Tavares y Vaz[9] proposed a technique where a second image with a fringe pattern orthogonal to the first one is used in order to eliminate the central component (background illumination) in frequency space. Chuen-Lin et al.[10] shows an approach based on a two-stage model: computation and extraction of a background-like quantity and local normalization of the fringes. As stated by Chuen-Lin,[10] the elimination of background illumination with a digital filter could filter out required phase information, and the orthogonal projection requires two images, but some errors could be generated when illumination varies with time.

Here, we present a single-stage method based on the computation of the envelopes of the intensity function, and derivation of background illumination and visibility from those. The method is clear, given that it handles quantities understandable from a physical point of view, and its implementation is straightforward. In Sec. 2, the underlying equations are presented; in Sec. 3, we discuss some details concerning the implementation of the method; Sec. 4 discusses the results of some tests on real and simulated interferograms and compares them with the results of Chuen-Lin et al. Finally, some conclusions are presented in Sec. 5.

2 Theoretical Basis

For the purposes of the present work, the intensity distributions considered are given by Ref. 11:

$$I(x,y) = A(x,y)(1 + B(x,y)\cos[\phi(x,y)]), \tag{1}$$

where the A function is the background illumination and B is the local visibility of the fringes. The ϕ function is the phase function. In order to perform the phase extraction, both A and B must be known, both representing unwanted irradiance variations arising from the nonuniform light due to features of the experimental setup in the optical test. One usual approach to remove background illumination is to use an image without fringe pattern in order to compute A,[11] given that usually it is determined by the illuminating conditions. Another approach is to take several pictures different interferograms and extract the information from there.[12] The approach we present here is a single image approach, which is useful because there are several circumstances where it is not possible to obtain more than one image, for example: analysis of dynamic interferograms, SAR satellite images, etc.

Let $\{x_L, y_L\}$ and $\{x_U, y_U\}$ the set of coordinates of the local minima and local maxima of the interferogram given by Eq. (1). The local fringe visibility is given by Ref. 11:

$$B(x,y) = \frac{E_U(x,y) - E_L(x,y)}{E_U(x,y) + E_L(x,y)} |\gamma_{12}(\tau)|, \tag{2}$$

where E_U is the upper envelope and E_L is the lower envelope and γ_{12} is a function related to the coherence of the waves. For our purposes here, we will take $|\gamma_{12}(\tau)| = 1$. The upper envelope is a smooth field that corresponds to the best fit in the least squares sense over the values of intensity in the coordinates $\{x_U, y_U\}$. Correspondingly, the lower envelope is the best fit in the least square sense over the values of intensity in the coordinates $\{x_L, y_L\}$.

Notice that over the set of local minima and maxima coordinates we have the following equations:

$$\begin{aligned} I(x_U, y_U) &= A(x_U, y_U)\left[1 + \frac{E_U(x_U, y_U) - E_L(x_U, y_U)}{E_U(x_U, y_U) + E_L(x_U, y_U)}\right] \\ &\approx E_U(x_U, y_U), \end{aligned} \tag{3}$$

$$\begin{aligned} I(x_L, y_L) &= A(x_L, y_L)\left[1 - \frac{E_U(x_L, y_L) - E_L(x_L, y_L)}{E_U(x_L, y_L) + E_L(x_L, y_L)}\right] \\ &\approx E_L(x_L, y_L), \end{aligned} \tag{4}$$

where the approximation is given in the least squares sense. It is easy to see that the following ansatz:

$$A(x,y) = \frac{E_U(x,y) + E_L(x,y)}{2}, \tag{5}$$

satisfies Eqs. (3) and (4) in the least squares sense.

What would Eq. (1) would look like in the best illumination conditions? In such a case, one should expect $E_U(x,y) = 1$ and $E_L(x,y) = 0$. Notice that 1 and 0 values for the upper and lower envelopes, respectively, are arbitrary (the intensity itself is in arbitrary units). Here, we choose those values for convenience on the analysis of the images. It follows that $A(x,y) = \frac{1}{2}$ and $B(x,y) = 1$. The corrected distribution function then would be given by:

$$i(x,y) = \frac{1}{2}(1 + \cos[\phi(x,y)]), \tag{6}$$

and it is related to the original distribution function via:

$$i(x,y) = \frac{1}{2}\left(1 + \frac{1}{B(x,y)}\left[\frac{I(x,y)}{A(x,y)} - 1\right]\right). \tag{7}$$

3 Implementation

This section explains in detail the implementation of the algorithm for processing of the interferometric images. The general idea of the method is to find the maxima and minima of the interference pattern and to use linear least squares (LLS) with, for example, Zernike polynomials to fit them and obtain the upper and lower envelope. After that, using Eqs. (2) and (5), compute the background illumination and the local visibility. The process is summarized in Fig. 1.

The preprocessing of the image consists of the removal of high-frequency noise components of the interferogram. The usual approach is to apply a low-pass filter with small convolution matrices.[1] Such filters are designed with some specific impulse response bear in mind. Some authors[10] have used the Wiener filter,[13] whose purpose is to reduce the amount of noise present in a signal in comparison with an estimation of the desired noiseless signal. Some algorithms compute such estimations locally in the neighborhood of the region being filtered, and because of this, they are usually termed as adaptive filters. In this work, we have used a smoothing process developed by us,[14] based on the fitting of the intensity distribution using Bessel functions of the first kind over slices of the interferogram. The discussion about the selection of filters is out of the scope of the present paper, but any approach should suffice as long as it helps to properly identify the maxima and minima of interference fringes.

The next step is the skeletonizing of the fringes. Within this context, it is important to clarify something: skeletonizing is different form band-tracking. In the band-tracking process, we can identify a set of coordinates (maxima) within an specifically numbered band, while skeletonizing is just the

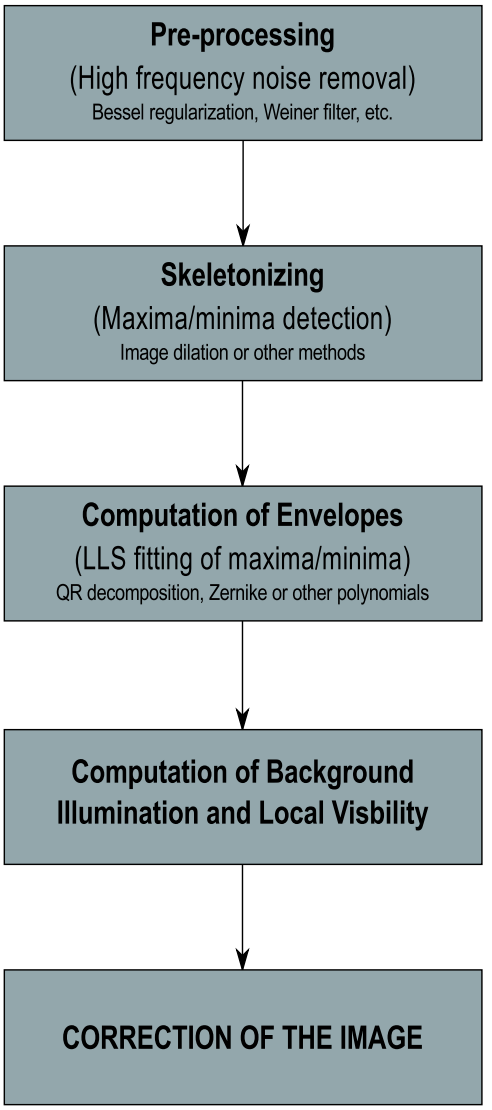

Fig. 1 Flow chart of the process.

detection of the maxima over the image. This can be performed by searching with algorithms based on line tracking, threshold comparison, or adaptive binarization.[1] There are very sophisticated approaches, such as algorithms that use the signal derived either from the image histogram or the cumulative distribution function to locate the peaks in the image histogram.[15] We obtained very good results using a simple peak detection algorithm based on image dilation by means of a plain structural Steel element.[16] The detection of the maxima is performed over the intensity distribution; as most algorithms are used for peak (maxima) detection, usually one can consider the auxiliary function $1 - I(x, y)$, where I have values in $[0, 1]$. This election is arbitrary and depends on the scale used for the intensity values.

The envelopes are smooth functions defined over the domain of the coordinates of the interferogram that are evaluated to the maxima (or minima) values of the intensity distribution in those coordinates, in the least squares sense. We have chosen to use LLS fitting of those values, but this is not the only possible approach: cubic splines or Lagrange interpolation polynomials are other options. We decided in favor of LLS because the implementation is largely known and algorithms are very efficient now-a-days. The problem is summarized in the following expression:

$$I(x_i, y_i) \approx \sum_{s=1}^{M} c_s A_s(x_i, y_i), \tag{8}$$

where I is the intensity distribution in the coordinates $\{x_i, y_i\}$ (i.e., the maxima or minima coordinates), c_s is a set of coefficients to be found, and A_s are the chosen basis functions. Such a system can be recast in the following matrix form:

$$\mathbf{A}\bar{c} = \bar{I}, \tag{9}$$

where $\mathbf{A}$ is a matrix whose columns represent each of the basis functions and the rows are those functions evaluated on each of the i-th coordinates; $\bar{c}$ is the row vector of the coefficients and $\bar{I}$ is the row vector of the intensity distribution at the desired coordinates. The $\mathbf{A}$ matrix is not square, and usually there are more points than basis functions; this means that the system is over-estimated, and it is solved using, for example, the Moore-Penrose generalized inverse.[17]

The condition number[18] of matrix $\mathbf{A}$ is a crucial quantitative indicator of the reliability of the computed coefficients, given that it is a measure of the error amplification factor when solving the least squares problem. If the matrix $\mathbf{A}$ is orthogonal, i.e., a matrix whose columns are orthogonal between them, its condition number is the lowest possible value: 1, no error amplification when computing the generalized inverse. In the general case, the matrix $\mathbf{A}$ will not be orthogonal over the discrete set of points under consideration for the selected basis functions. In the cases where there are problems with the computation of the coefficients because of large condition numbers of $\mathbf{A}$, the matrix can be factorized using $\mathbf{QR}$ decomposition,[18] which allows the representation in a new basis set with different coefficients and an orthogonal matrix.

For our purposes, we have selected the Zernike polynomials as our basis functions, given that we are dealing with circular domains. Each basis set have specific domains, so the coordinates should be scaled accordingly. When dealing with domains with different geometries, other basis should be considered. For example, for Cartesian domains, a good basis set should be Chebyshev polynomials.[19] The Zernike polynomials are invariant in form with respect to rotation of axes around the origin.[11] In other words, we are dealing for polynomials in the following form:

$$Z_n^m = e^{\mathrm{im}\theta} R_n^m(\rho), \tag{10}$$

where the term $e^{\mathrm{im}\theta}$ is the usual Euler symbol, an orthogonal function with index m that close over itself after a 2π revolution. The R_n^m polynomial is usually know as the radial Zernike polynomial of degree n, and contains no powers of degree lower than $|m|$; also, R_n^m is an even or odd polynomial according as m is even or odd. Then, the total number of terms up to degree N is $(N + 1)(N + 2)/2$.

The degree required for the correct fitting of the envelopes depends on the irregularity of the background illumination: a higher degree is required for more irregular illuminating conditions. This is also related to the following rule of thumb: for any LLS problem, the number of sampled points (in this case, intensity values), must be at least the number of terms considered in the expansion.

It is also important to consider the distribution of the points along the domain; the values of the envelope functions in the intermediate coordinates between the sampling points are interpolated according to the respective Zernike expansion, while the values of the envelope functions for coordinates not between sampling points are extrapolated, hence being less meaningful and subject to greater uncertainty. For example, for an interferogram with only one bright vertical fringe spanned through the whole domain, the corresponding locus of the maxima would be a line along the center of the domain (and probably no loci for the minima). This interferogram would sample the upper envelope in the vertical direction, but brings no information in the horizontal direction; at the same time, it may not bring any information for the lower envelope, providing poor local visibility and background illumination functions. Following this argument, it is easy to see that a higher number of resolvable fringes in the interferogram allows a better fitting of the envelope functions, thus allowing a better correction of the image.

The last step in the implementation is the computation of the local visibility, Eq. (2), and the background illumination, Eq. (5). The correction of the image is then straightforward using Eq. (7).

Various authors have discussed about the meaning of an adequate management of these two quantities: Takeda explains how to separate the carrier frequency of the unwanted background variation via spectral analysis, in order to succeed in determining the phase;[6] more recently, Chuen-Lin et al. proposed a new method for fringe normalization by Zernike polynomials fitting to cancel the background illumination and local normalization in the regions near the maxima and minima of the modified pattern, with the purpose of enhancement of the contrast fringe to separate the carrier frequency as proposed by Takeda.[10] Other works[9] have tried to mitigate the effect of the

unwanted illumination and improve the contrast of the fringes and also eliminating the high-frequency to determine the phase using Takeda, because the Takeda method is the simplest and more effective method for shape measurement.

4 Results and Discussion

In this section, we implement the proposed method to correct real interferograms that exhibit significant nonuniform illumination. According to Takeda,[6] the fringe pattern in the Fourier space is compounded by unwanted background and the carrier frequency plus frequency associated with noise . On the Takeda proposal, the carrier frequency is isolated and used to obtain the phase. In some cases, this frequency is overlapping with the rest of the other, making the isolation more difficult.[9,10,12] We will not be able to develop the whole process to extract the phase in this paper, but we show how much the interferogram images can be enhanced suppressing the intensity background computed by our method and normalizing the contrast.

In the Fig. 2(a), an experimental interferogram obtained from a Ronchi test is shown. This is a lateral shearing interferogram and can be appreciated a well defined carrier frequency. On the other hand, the Fig. 2(b) shows the same interferogram after the background intensity suppression and the normalization of the visibility, Eq. (7). The differences between the images are clear to the eye, in terms on contrast of the fringes as well as homogeneity in the illumination.

A more quantitative picture can be seen in Fig. 3, where a row of the original interferogram, Fig. 2, is displayed as a red continuous line; the black continuous lines are the computed envelopes and the dashed blue line is the intensity of the corrected interferogram. A full overview of the process is presented in the Fig. 4: Fig. 4(a) shows the fringe visibility computed by means of Eq. (2) from the original interferogram; Fig. 4(b) shows the background illumination computed by means of Eq. (5). Both results were used in order to process the image; the Fig. 4(c) is a three-dimensional (3-D) mesh of the original interferogram, and Fig. 4(d) is a 3-D mesh of the corrected interferogram.

Recently, Chuen-Lin et al.[10] have suggested the use of Zernike polynomials to compute a quantity similar to background illumination via least squares fitting over the intensity function. This quantity is subtracted directly to the intensity function. Then, the high-frequency noise is filtered using adaptive Wiener filter to smooth the image. Finally, fringe

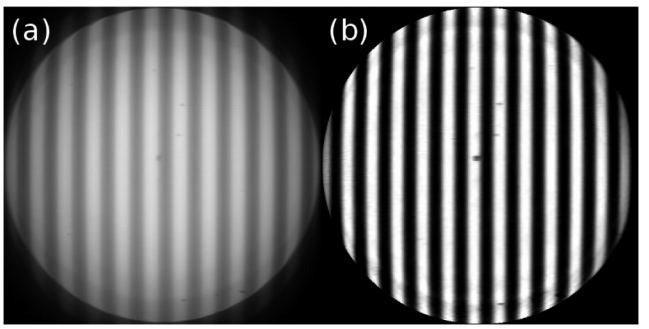

Fig. 2 (a) Original interferogram obtained from a Ronchi test. (b) Corrected interferogram by means of background illumination regularization.

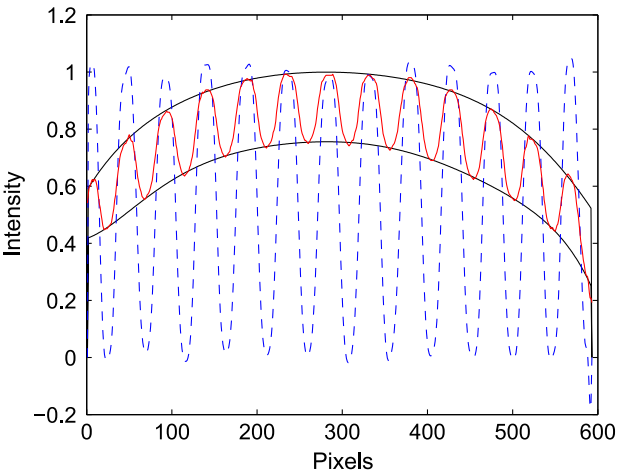

Fig. 3 Slice of the intensity distribution of the interferogram of Fig. 2. The red continuous line is the intensity of the original image after of a smoothing process. The black continuous lines are the computed envelopes. The dashed blue line is the intensity of the corrected interferogram.

normalization should be carried out using a local region (basically defining it as the locus of the fringe) contrast modulation. The amplitude modulation process is implemented as follows:

(1) Plus and minus regions are created from the values of the images pixels, after the background illumination had been removed.

(2) Local maximum in the plus region and local minimum in the minus region are computed.

(3) Finally, each of the regions are divided by the absolute value of local maximum and minimum, respectively.

This method had proved to be quite efficient, but it has the drawback of being somewhat confusing because it does not resemble the physical quantities involved in the interference process. It may seem that our proposal is very similar to the one proposed by Chuen-Lin et al., but it posses some key differences: on one hand, the least squares fitting is performed only over the maxima (or minima) of the pattern, allowing a suitable computation of the upper (or lower) envelope. Based on these functions, the envelopes, the computation of the background illumination, and visibility is performed, and using both of them, the correction is executed. This allows the preservation of the shape of the fringes, contrary to the proposal of Chuen-Lin, where the local normalization may change them. Another key difference between the approaches is the preprocessing of the images: while Chuen-Lin uses the adaptive Wiener filter, the recommendation here is to use a smoothing process using Bessel functions,[14] because it has been proved that it works excellent with interferogram images, due to the resemblance between the Bessel function and the interference pattern along one direction.

In order to compare the two methods, the process was applied to an interferogram taken under very poor illumination conditions. The Fig. 5 shows the results using both approximations: Fig. 5(a) exhibits the plots of the intensity

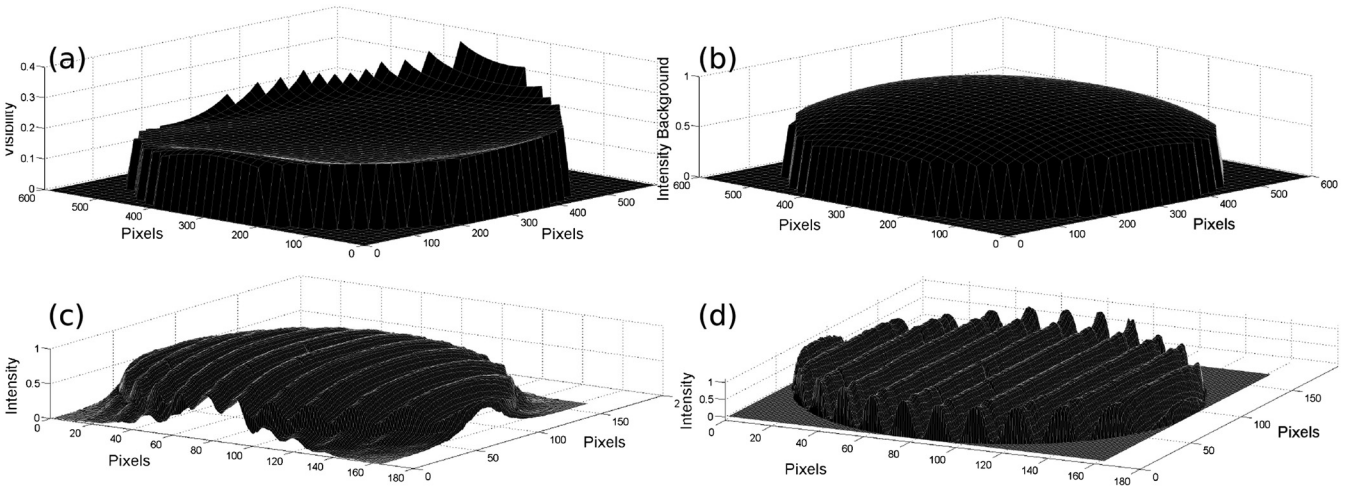

Fig. 4 (a) Fringe visibility computed by means of Eq. (2) from the interferogram of Fig. 2. (b) Background illumination computed by means of Eq. (5). (c) 3-D mesh of the interferogram of Fig. 2. (d) 3-D mesh of the corrected interferogram of the Fig. 2.

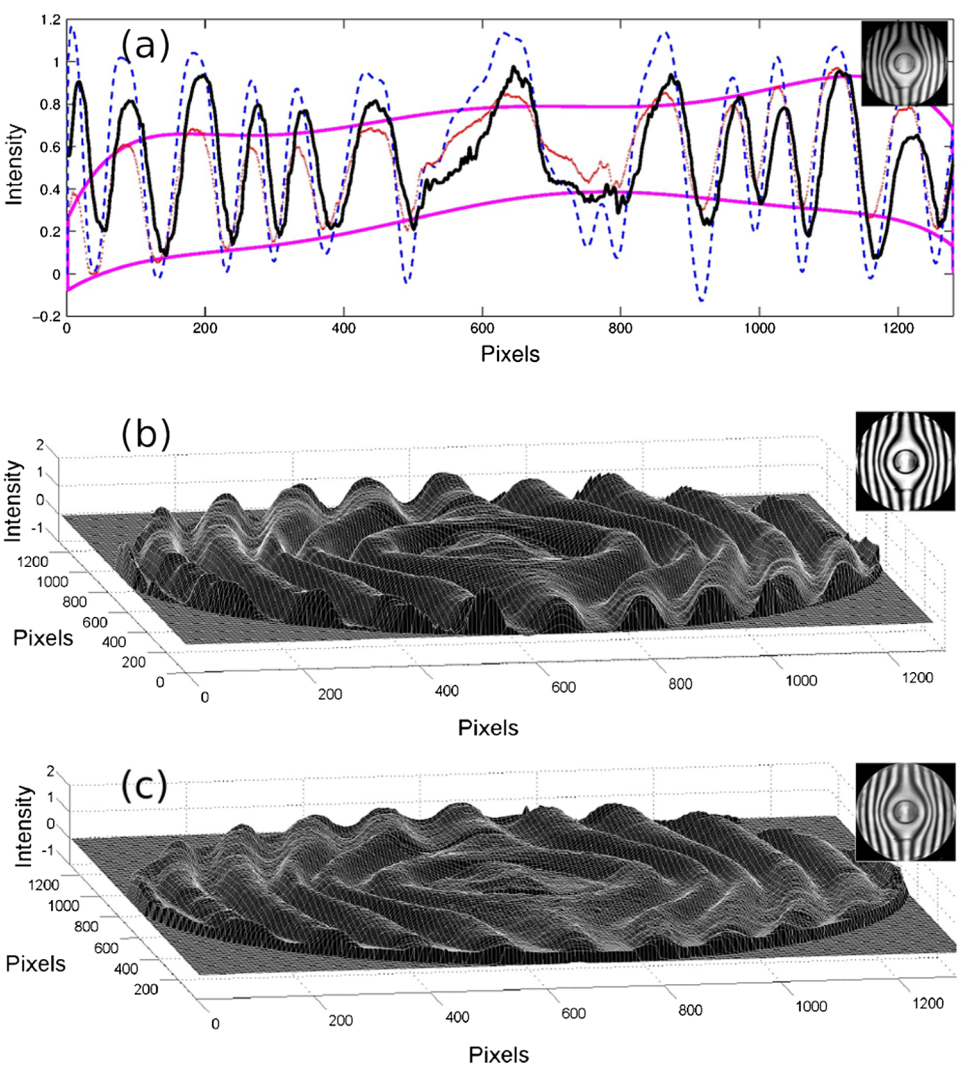

Fig. 5 (a) Intensity function for a slice of the original and processed interferograms; the original image in red circles; the black continuous line are the results obtained using Chuen-Lin et al. approximation,[10] and in blue dashed line the results using the method presented here. The purple continuous line are the computed envelopes. (b) and (c), are a 3-D mesh for our proposal and Chuen-Lin et al. aproximation, respectively. The inset are the interferogram of : (a) Original, (b) our method and (c) Chuen-Lin et al. aproximation.

function for a slice of the original and processed interferograms; the original image in red circles; the black continuous line are the results obtained using Chuen-Lin et al. approximation,[10] and in blue dashed line, the results using the method presented here. The purple continuous line are the computed envelopes. The inset in the Fig. 5(a) displays the original interferogram.

It can be observed that the strong nonuniformity of the illuminating field, even when the method could not correctly compute the envelopes for the intensity distribution, it performed somewhat better than the one proposed by Chuen-Lin et al. Usually, software with image capabilities such as Matlab truncates values higher than one or lower than zero; this "visually" improves the final result, at least from a human point of view. Besides, the fringe shape (width) is preserved using our approach. In Fig. 5(b) and 5(c), we can see a 3-D mesh for each processed image (with their respective picture in the inset); the difference between the oscillations in the intensity functions is clearly seen, where larger, better defined oscillations represent images with better contrast.

4.1 *Performance Testing*

In order to test the performance of the method in "complicated" situations, we simulated an interferogram using a pattern with vortices,[20] which is an interference of two waves with the following phase functions:

$$\phi_1 = \pi \sin(6\theta), \tag{11}$$

$$\phi_2 = 5\theta + 50\rho, \tag{12}$$

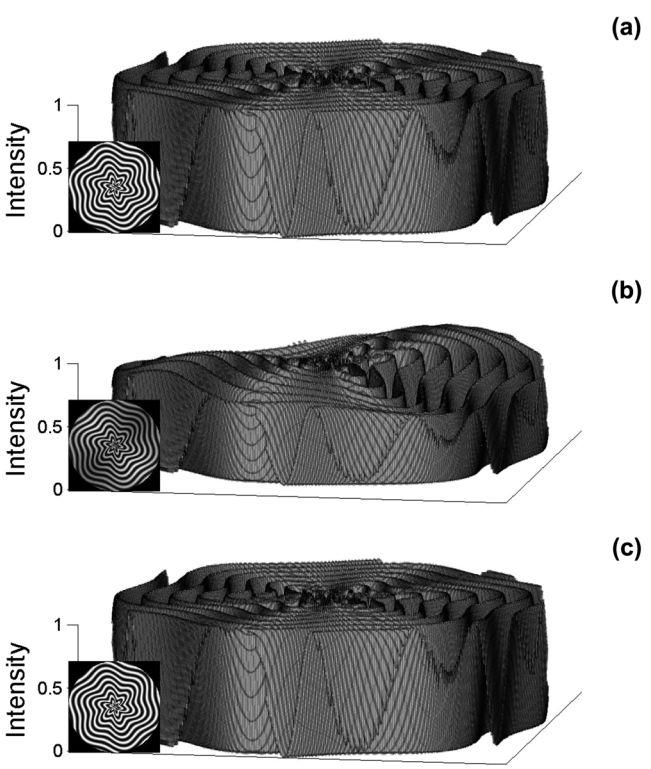

Fig. 6 Regularization of a vortex interferogram. (a) Original (simulated) interferogram. (b) Interferogram with complicated uneven illumination conditions. (c) Processed interferogram with regularization method. The insets show the interference pattern in each case.

in polar coordinates. The interference pattern can be seen on the inset of Fig. 6(a). This pattern is interesting because the fringes have very complicated geometries. For simulating the unfavorable illumination conditions, the following A and B functions were proposed:

$$A(\theta,\rho) = 0.4 + 0.1 \sin[\pi\rho \cos(\theta)] \sin[\pi\rho \sin(\theta)], \tag{13}$$

$$B(\theta,\rho) = \exp[-(\rho/2)^2]. \tag{14}$$

Figure 6(a) shows a mesh of the vortex interference image, and the modified image with the uneven background illumination can be easily appreciated on Fig. 6(b). The regularized image, result of the process, can be seen in Fig. 6(c). Also, a plot of the whole computed background illumination can be seen in Fig. 7(a), and the local visibility can be seen in Fig. 7(b). The A and B functions were intentionally chosen to not being trivially represented by Zernike polynomials.

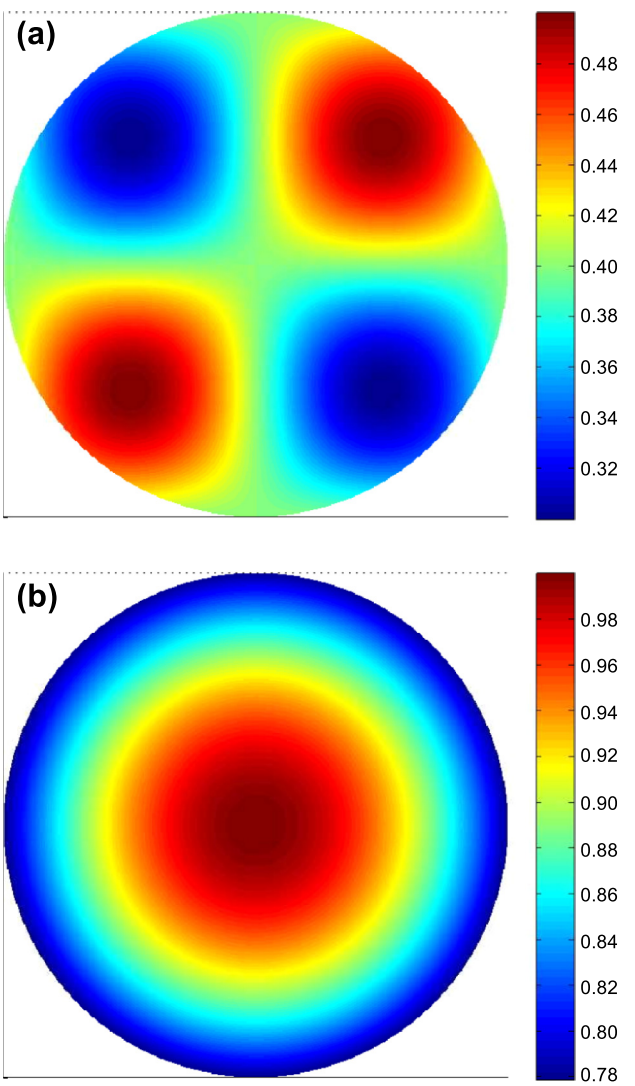

Fig. 7 (a) Background and (b) local visibility computed from the vortex interferogram.

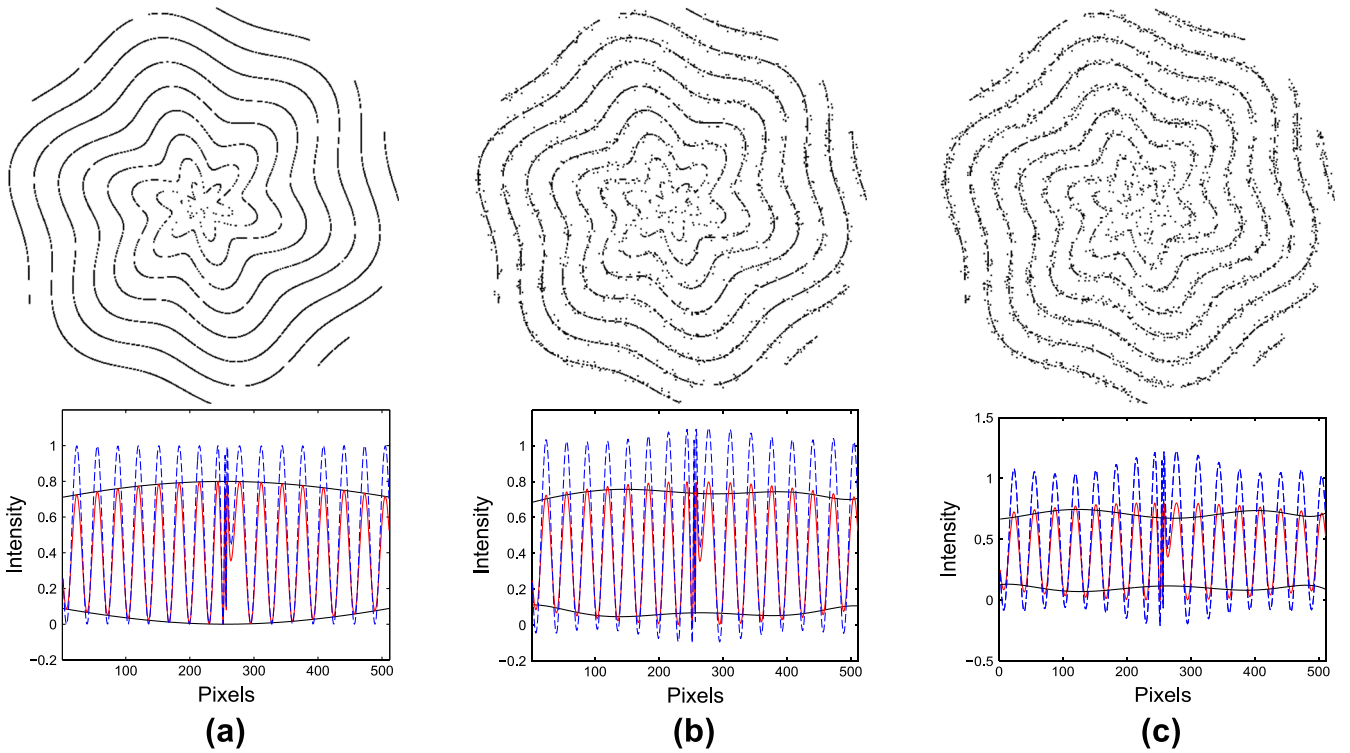

Fig. 8 Effect of the incorrect localization of the extrema in the regularization process. (a) Fraction of incorrectly localized extrema: 1%. (b) Fraction of incorrectly localized extrema: 30%. (c) Fraction of incorrectly localized extrema: 50%. In all of the plots, the maximum pixel deviation is 5.

In order to analyze the effect of noise or incorrect localization of the extrema in the interference image, we designed a test, where a fraction of the maxima and minima of the image are incorrectly identified, shifting randomly its correct position some pixels in a random direction horizontally and vertically. The Fig. 8 shows three examples of such a test. In all of the examples, the maxima (and minima) can change their position up to five pixels horizontally and up to five pixels vertically, with random direction (left and right or up and down, respectively).

The Fig. 8(a) shows the locus of the minima and the plot for the center vertical slice of the regularization. It can be seen that a small fraction of noise (1%) in the localization of minima and maxima have no repercussion on the process and the interferogram can be properly corrected. As the fraction of noise is raised, the process executes less efficiently, as can be seen in Fig. 8(b), with a fraction of 30%, and Fig. 8(c), with a fraction of 50%.

It is specially important to address something here: the wrong localization of the extrema is equivalent to have a noisy image. Noise in the interferogram produces false peaks (extrema) that can be identified by the skeletonizing algorithm as extrema of the intensity distribution. Inaccurate localization of the maxima of the interferogram leads to incorrect computation of the envelopes, and then, to incorrect A and B functions.

In order to quantify these deviations, we compute a residual function for the corrected interferogram as follows:

$$R = \frac{1}{2}\left(\sqrt{\sum_{i}^{N_{\max}}(I_i^{\max}-1)^2} + \sqrt{\sum_{i}^{N_{\min}}(I_i^{\min}-0)^2}\right), \qquad (15)$$

where $N_{\max}$ and $N_{\min}$ is the total number of maxima and minima detected, respectively; $I_i^{\max}$ and $I_i^{\min}$ are the i-th maxima and minima detected, respectively. This residual is a mean between the standard deviation of the maxima with respect to the ideal maximum value (1) and the standard deviation of the minima with respect to the ideal minimum value (0), of the corrected interferogram. The results for the test can be seen on Fig. 9. The residual was computed for the same image, varying the amount of incorrectly located extrema, for several values of the maximum pixel deviation, and averaging the residual for 10 interferograms. Empirically, the region below $R = 1$ is of acceptable tolerance for deviations.

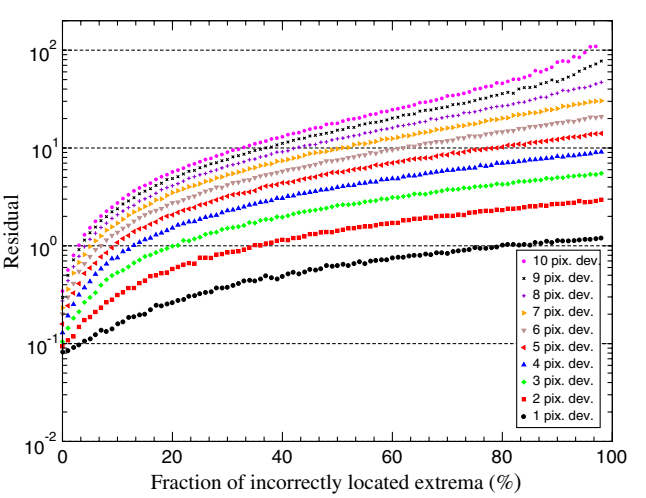

Fig. 9 Residual as a function of the fraction of incorrectly located extrema, for several values of the maximum pixel deviation.

5 Conclusions

A new method to suppress the background illumination and to control the local visibility in interferometric images was presented. This new approach involves physical-like quantities, which are by tradition the main parameters for the study of interferometry, making the process of understanding much more natural and obvious. The background illumination and visibility can affect the correct phase extraction, therefore must to be controlled by manipulating the experimental conditions and/or by computational treatment.

Finding the maxima and minima of the interference pattern and using them for LLS with Zernike polynomials, the upper and lower envelope are computed. Using Eqs. (2) and (5), the background illumination and the local visibility are achieved, then the correction is performed. This proposal seems similar to the Chuen-Lin et al. approximation, but the differences are remarkable: first of all, in the proposal of this work, the least squares fitting is performed only over the maxima (or minima) of the pattern, allowing a suitable computation of the upper (or lower) envelope; on the other hand, the other work proposed use Zernike polynomial to compute a quantity similar to background illumination via least squares fitting over whole the intensity function. The other big difference between the methods is how fringe normalization is carried out. Chuen-Lin et al. suggest to distinguish plus and minus regions (for fringe patterns defined with positive and negative values of intensity) after the background illumination had been removed to compute local maximum in the plus region and local minimum in the minus region and finally each of the regions are divided by the absolute value of local maximum and minimum, respectively. In this paper, the best illumination conditions are achieved using the Eq. (7), making some changes to the original interferometric image until the conditions are met, this means, introducing into the equation calculated values of visibility $B(x, y)$ and background $A(x, y)$.

The results showed how much the interferometric image can be enhanced when the method proposed is implemented. Since the visibility and background can be corrected using this method, then the extraction of the phase or Fourier analysis can be implemented with higher success avoiding problems such as the overlapping of the Fourier components. We have shown two key factors in the success of the application of the method: on one hand, the number of detected extrema should be at least $(N+1)(N+2)/2$, where N is the highest degree in the Zernike polynomials considered, which is a small number in comparison to the number of points in a typical interferogram; and on the other hand, those extrema should accurately detected. This method provides a simple, elegant, rapid, and natural process to enhance the contrast of the interferometric image, and prepare it for future studies.

Acknowledgments

This work is funded by CONACYT, Mexico. Romero-Antequera and Penalver would like to thank CONACYT for scholarships with numbers: 223982 and 23980, respectively.

References

1. D. Malacara, M. Servín, and Z. Malacara, *Interferogram Analysis for Optical Testing*, 2nd ed., Taylor & Francis Group, Boca Raton, FL (2005).
2. P. J. Tavares and M. A. Vaz, "Linear calibration procedure for the phase-to-height relationship in phase measurement profilometry," *Opt. Commun.* **274**(2), 307–314 (2007).
3. E. Stoykova, J. Harizanova, and V. Sainov, "Pattern projection with a sinusoidal phase grating," *EURASIP J. Adv. Sig. Process.* **2009**, 351626 (2009).
4. G. Rajshekhar, S. S. Gorthi, and P. Rastogi, "Polynomial wigner-ville distribution-based method for direct phase derivative estimation from optical fringes," *J. Opt. A Pure Appl. Opt.* **11**(12), 125402 (2009).
5. R. Restrepo, N. Uribe-Patarroyo, and T. Belenguer, "Improvement of the signal-to-noise ratio in interferometry using multi-frame high-dynamic-range and normalization algorithms," *Opt. Commun.* **285**(5), 546–552 (2012).
6. M. Takeda, H. Ina, and S. Kobayashi, "Fourier-transform method of fringe-pattern analysis for computer-based topography and interferometry," *J. Opt. Soc. Am.* **72**(1), 156–160 (1982).
7. J. A. Quiroga, J. A. Gomez Pedrero, and A. Garcia-Botella, "Algorithm for fringe pattern normalization," *Opt. Commun.* **197**(1–3), 43–51 (2001).
8. J. A. Quiroga and M. Servin, "Isotropic n-dimensional fringe pattern normalization," *Opt. Commun.* **224**(4–6), 221–227 (2003).
9. P. J. Tavares and M. A. Vaz, "Orthogonal projection technique for resolution enhancement of the fourier transform fringe analysis method," *Opt. Commun.* **266**(2), 465–468 (2006).
10. C.-L. Tien, S.-S. Jyu, and H.-M. Yang, "A method for fringe normalization by zernike polynomial," *Opt. Rev.* **16**(2), 173–175 (2009).
11. M. Born and E. Wolf, *Principles of Optics*, Cambridge University Press, Cambridge, United Kingdom (1999).
12. P. K Rastogi Ed., *Photomechanics*, Springer, Berlin, Germany (1999).
13. J. S. Lim, *Two-Dimensional Signal and Image Processing*, Prentice Hall Inc., Englewood Cliffs, NJ (1990).
14. D. H. Penalver, D. L. Romero-Antequera, and F. Granados-Agustin, "Interferogram smoothing and skelotonizing using bessel functions of the first kind," *Opt. Eng.* **51**(4), 045601 (2012).
15. M. I. Sezan, "A peak detection algorithm and its application to histogram-based image data reduction," *Comput. Vision. Graph. Image. Process.* **49**(1), 36–51 (1990).
16. Y. Nativ, "Local maxima detection using image dilation. this code is publicly available at matlab central file exchange website.," September 2007, http://www.mathworks.com/matlabcentral/fileexchange/14498-local-maxima-minima.
17. A. Albert, *Regression and the Moore-Penrose Pseudoinverse*, Academic Press, Inc., New York, NY (1972).
18. C. L. Lawson and R. J. Hanson, *Solving Least Squares Problems*, Society for Industrial and Applied Mathematics. Republished by Prentice Hall, Englewood Cliffs, NJ (1974).
19. F. Marcellán and W. Van Assche, *Orthogonal Polynomials and Special Functions: Computation and Applications*, Lecture Notes in Mathematics, Springer, The Netherlands (2006).
20. P. Senthilkumaran, J. Masajada, and S. Sato, "Interferometry with vortices," *Int. J. Opt.* **2012**, 517591 (2012).

David L. Romero-Antequera received his BS degree in physics at the University of Carabobo, Venezuela, in 2005. He got his MS degree in optical science from the National Institute for Astrophysics, Optics and Electronics (INAOE is the acronym in Spanish) in 2008. Currently, he is a PhD student at INAOE. Posses strong background in programming, specifically in simulation of electromagnetic phenomena and nonlinear optimization problems. His last research interest are about photonic crystal, structured media, and phase unwrapping problems.

Dayana H. Penalver is a member of SPIE, currently a PhD student in the National Institute for Astrophysics, Optics and Electronics (INAOE is the acronym in Spanish) in Puebla, Mexico. She received her BS degree in physics in 2006 from the Carabobo University in Venezuela, and MS degree in Optical Science in 2008 from INAOE. She has experience in optical testing in the laboratory, and simulations for development of optical systems. She also worked in fit of multidimensional experimental data of power spectral density for validation and modification of the general theory of Harvey-Shack.

Fermín-Salomón Granados-Agustín is a researcher in the Optics Department of the National Institute of Astrophysics, Optics, and Electronics INAOE, México. He received his BS degree in physics from the National University of Mexico UNAM, in 1993. He received his MS degree and PhD degree in optics, respectively, in 1995 and 1998, both from the INAOE. He is a national researcher for the National System of Researches, Mexico. He held a postdoctoral position at the Mirror Lab of the Steward Observatory at the University of Arizona, in 1999. He has been the head of the optical shop at the INAOE, since 2005. His research interests include optical information, interferometric optical testing, and instrumentation.

Javier Sánchez-Mondragón is researcher at the National Institute for Astrophysics, Optics and Electronics (1990) and previously at the Center for Research in Optics in Leon Guanajuato (1980 to 1990). He is member of the National System of Researchers at the level III (Highest), fellow of the Optical Society of America, member of the National Academy of Sciences, member, prize and former president of the Mexican Academy of Optics. He graduated from the Department of Physics of the University of Rochester (1980) and obtained a BS degree in physics from the Autonomous National University of Mexico (1974).